Viscously damped acoustic waves with the lattice Boltzmann method

By Erlend Magnus Viggen

Acoustics Group, Dept. of Electronics and Telecomm., Norwegian University of Science and Technology, O. S. Bragstads Plass 2, 7034 Trondheim, Norway

Acoustic wave propagation in lattice Boltzmann BGK simulations may be analysed using a linearization method. This method has been used in the past to study propagation of waves which are viscously damped in time, and is here extended to also study waves which are viscously damped in space. Its validity is verified against simulations, and the results are compared with theoretical expressions. It is found in the infinite resolution limit $k \to 0$ that the absorption coefficients and phase differences between density and velocity waves match theoretical expressions for small values of $\omega\tau_\nu$, the characteristic number for viscous acoustic damping. However, the phase velocities and amplitude ratios between the waves increase incorrectly with $(\omega\tau_\nu)^2$, and agree with theory only in the inviscid limit $k \to 0, \omega\tau_\nu \to 0$. The actual behaviour of simulated plane waves in the infinite resolution limit is quantified.

Keywords: Lattice Boltzmann, wave propagation, computational aeroacoustics

1. Introduction

In a seminal article, Lighthill showed how flow fields may act as acoustic sources [1], thereby planting the seed for the scientific field now known as aeroacoustics. The related field of computational aeroacoustics (CAA) has been studied since the 1980s, and two main approaches of CAA have been identified:

The hybrid approach, where the flow and acoustic fields are found separately. The flow field is analysed to find the acoustic source strength of the flow, which is then used to compute the acoustic field in the surrounding domain.

The direct approach, where the acoustic field comes out as a natural part of a numerical solution to the compressible Navier-Stokes equation.

One important weakness of the hybrid approach is its inability to simulate the feedback of the acoustic field on the flow field. This means that it is not usable in cases where this feedback is critical to the process of sound generation, such as in the singing risers problem currently studied in the natural gas industry [2]. It is also difficult to capture complex geometries with this method.

The direct approach has no such problems, but traditional numerical simulations of the compressible Navier-Stokes equation are far more complex and demanding than hybrid methods. It is therefore our hope that the lattice Boltzmann method (LBM) can be used for direct CAA. Compared to traditional methods, the LBM is straightforward to implement. It is also an explicit method which can be parallellized with a nearly linear speedup in number of processors.

There exists a large body of work which validates the LBM as a useful tool for simulations of incompressible flow [3]. However, it has been shown mathematically that the LBM may also be used for solving the compressible Navier-Stokes equation [4], albeit with spurious $\mathcal{O}(\mathrm{Ma}^3)$ terms which limit its applicability to small Mach numbers and cause incomplete Galilean invariance.

To ascertain whether the LBM may become a useful tool for CAA, we need a better picture of the acoustic behaviour of the method. This article will focus on viscous damping of acoustic waves. In §2, the theory of this behaviour is described. §3 describes a method of linearization analysis which can be applied to study this behaviour in the LBM. The method is validated in §4, and is then used to compare the behaviour of LB-simulated waves with theoretically expected behaviour.

2. Theoretical background

When performing the Chapman-Enskog analysis on the LBM, certain assumptions must be made to retrieve the compressible Navier-Stokes equation. First, one assumes that the Mach number is sufficiently low that the aforementioned spurious terms can be neglected. Second, one assumes isothermal compression, so that the absolute pressure and density p and ρ are linked through the thermodynamic speed of sound $c_s = 1/\sqrt{3}$ as $p = c_s^2 \rho$. These assumptions fit well with those made in linear acoustics: Low Mach number and adiabatic compression, so that the off-equilibrium pressure and density p' and ρ' are linked as $p' = c_s^2 \rho'$.

One result of the Chapman-Enskog analysis is that the kinematic shear and bulk viscosities for the BGK collision operator are given through the relaxation time τ as respectively

$$\nu = c_s^2 \left(\tau - 1/2\right), \tag{2.1a}$$

$$\nu' = 2\nu/3. \tag{2.1b}$$

This constant ratio between bulk and shear viscosities make it impossible to perform simulations of fluids with correct transport coefficients without resorting either to extended LB methods (e.g. [4]), or to another type of collision operator such as the Multiple Relaxation Time (MRT) operator (e.g. [5]). Both these choices would allow us to set bulk and shear viscosity independently.

(a) Solutions to the lossy wave equation

Conservation of mass and momentum are expressed through the continuity and compressible Navier-Stokes equations, which relate density ρ, pressure p, and particle velocity $\mathbf{u}$,

$$\frac{\partial \rho}{\partial t} = -\nabla \cdot (\rho \mathbf{u}), \tag{2.2a}$$

$$\rho \frac{D\mathbf{u}}{Dt} = -\nabla p + \rho \left(\frac{4}{3}\nu + \nu'\right) \nabla(\nabla \cdot \mathbf{u}) - \rho \nu \nabla \times \nabla \times \mathbf{u}. \tag{2.2b}$$

Assuming low Mach number, adiabatic compression, and sufficient distance to boundaries, it may be shown similarly to ref. [6] that this implies a lossy wave

equation,

$$\left(1 + \tau_\nu \frac{\partial}{\partial t}\right)\nabla^2 p - \frac{1}{c_s^2}\frac{\partial^2 p}{\partial t^2} = 0, \tag{2.3}$$

where $\tau_\nu = (\frac{4}{3}\nu + \nu')/c_s^2$ is the viscous relaxation time. Inserting from eq. 2.1, we find for the LBM that $\tau_\nu = 2\tau - 1$. From the extended analysis of Hamilton & Morfey [7], we see that eq. 2.3 is correct up to second order in Mach number and $\omega\tau_\nu$ if the effects of thermal conduction and molecular relaxation are neglected.

In one dimension, this equation implies general damped wave solutions in pressure, density, and particle velocity,

$$\hat{p}(x,t) = p_0 + \hat{p}'\mathrm{e}^{\mathrm{i}(\hat{\omega}t - \hat{k}x)}, \tag{2.4a}$$

$$\hat{\rho}(x,t) = \rho_0 + \hat{\rho}'\mathrm{e}^{\mathrm{i}(\hat{\omega}t - \hat{k}x)}, \tag{2.4b}$$

$$\hat{u}(x,t) = \hat{u}'\mathrm{e}^{\mathrm{i}(\hat{\omega}t - \hat{k}x)}, \tag{2.4c}$$

where a hat implies a complex quantity, and $\hat{\omega} = \omega' + \mathrm{i}\alpha_t$ and $\hat{k} = k' - \mathrm{i}\alpha_x$ are complex angular frequency and complex wavenumber respectively. α_t and α_x are the temporal and spatial absorption coefficients, while the real parts ω' and k' are linked through a phase velocity, $c_p = \omega'/k'$. By comparison, we have in lossless media that $\hat{k} = k$, $\hat{\omega} = \omega$, and $c_p = \omega/k = c_s$.

Two important special cases are temporal damping (when $\hat{k} = k$) and spatial damping (when $\hat{\omega} = \omega$). In both cases, properties of the waves can be found by inserting eq. 2.4a into eq. 2.3. For spatially damped waves, we thus find

$$\frac{\alpha_x}{k} = \sqrt{\frac{\sqrt{1 + (\omega\tau_\nu)^2} - 1}{2 + 2(\omega\tau_\nu)^2}}, \quad \frac{k'}{k} = \sqrt{\frac{\sqrt{1 + (\omega\tau_\nu)^2} + 1}{2 + 2(\omega\tau_\nu)^2}}, \quad \frac{c_p}{c_s} = \sqrt{\frac{2 + 2(\omega\tau_\nu)^2}{\sqrt{1 + (\omega\tau_\nu)^2} + 1}}, \tag{2.5}$$

whereas for temporally damped waves we find

$$\alpha_t/\omega = \omega\tau_\nu/2, \qquad \omega'/\omega = \sqrt{1 - (\omega\tau_\nu)^2/4}, \qquad c_p/c_s = \sqrt{1 - (\omega\tau_\nu)^2/4}. \tag{2.6}$$

These expressions only depend on the dimensionless quantity $\omega\tau_\nu$, which may be seen as a characteristic dimensionless number for the effect of viscous acoustic damping. Spatially damped waves occur whenever a wave is radiated from an acoustic source in an absorbing medium, and is the type commonly encountered in nature.

Early numerical studies of wave propagation with the LBM focused on temporally damped waves, propagating a single wavelength in a periodic system [8]. Later numerical studies have taken spatial damping into account as well [9].

(b) Linearization of conservation equations

By inserting the damped wave solutions in eq. 2.4 into the conservation equations in eq. 2.2 under the linearizing assumptions that the wave amplitudes $\hat{p}'$, $\hat{\rho}'$, and $\hat{u}'$ are very small, we may reduce these equations to relations between the complex wave amplitudes,

$$\hat{u}'/\hat{\rho}' = \hat{\omega}/\rho_0\hat{k}, \tag{2.7a}$$

$$\hat{p}'/\hat{u}' = \rho_0\hat{\omega}/\hat{k} - \mathrm{i}\rho_0\hat{k}\left(4\nu/3 + \nu'\right). \tag{2.7b}$$

The absolute values of these ratios indicate the amplitude ratios between the waves, while the complex phases describe the phase difference between them. For temporal and spatial damping, we may use expressions from eqs. 2.5 and 2.6.

3. Linearization analysis of lattice Boltzmann

The acoustic behaviour of LB may be analysed by performing a similar linearization [4,5]. We assume that we have a rest state F_i^{eq} of density ρ_0 with a fluctuation $\hat{f}_i$ on top. We assume this to be on a general complex one-dimensional wave form,

$$\hat{f}_i(x,t) = \hat{h}_i e^{i(\hat{\omega}t - \hat{k}x)}. \tag{3.1}$$

If this wave is very small, we may linearize the equilibrium distribution,

$$\hat{f}_i^{\text{eq}} + F_i^{\text{eq}} = \hat{\rho}t_i \left[1 + 3\hat{u}c_i + 9(\hat{u}c_i)^2/2 - 3\hat{u}^2/2 \right],$$
$$\hat{f}_i^{\text{eq}} \simeq t_i \left[(\hat{\rho} - \rho_0) + 3\rho_0 \hat{u} c_i \right]. \tag{3.2}$$

In this small-amplitude limit, the aforementioned $\mathcal{O}(\text{Ma}^3)$ errors disappear.

While this behaviour could be examined for a number of different lattices, we will follow ref. [10] and limit ourselves to the D1Q3 lattice, which is a one-dimensional projection of a number of common lattices (D2Q9, D3Q15, D3Q19, and D3Q27). Thus, plane waves in D1Q3 are equivalent with plane waves along any main axis of these other lattices. The D1Q3 lattice is given by velocities $[c_-, c_0, c_+] = [-1, 0, 1]$ and weights $[t_-, t_0, t_+] = [1/6, 2/3, 1/6]$.

With density and momentum given as

$$\hat{\rho}(x,t) = \rho_0 + \sum_i \hat{f}_i(x,t) = \rho_0 + (\hat{h}_- + \hat{h}_0 + \hat{h}_+)e^{i(\hat{\omega}t - \hat{k}x)}, \tag{3.3a}$$

$$\rho_0 \hat{u}(x,t) = \sum_i c_i \hat{f}_i(x,t) = (\hat{h}_+ - \hat{h}_-)e^{i(\hat{\omega}t - \hat{k}x)}, \tag{3.3b}$$

we find a post-collision distribution

$$\hat{g}_i(x,t) = \hat{f}_i(x + c_i, t + 1) = \left(1 - \frac{1}{\tau} \right) \hat{f}_i(x,t) + \frac{1}{\tau} \hat{f}_i^{\text{eq}}(x,t)$$
$$= \left\{ \left(1 - \frac{1}{\tau} \right) \hat{h}_i + \frac{t_i}{\tau} \left[\hat{h}_- + \hat{h}_0 + \hat{h}_+ + 3c_i(\hat{h}_+ - \hat{h}_-) \right] \right\} e^{i(\hat{\omega}t - \hat{k}x)}. \tag{3.4}$$

If we for simplicity assume x and t such that $e^{i(\hat{\omega}t - \hat{k}x)} = 1$, we find

$$\hat{f}_i(x, t+1) = \hat{g}_i(x - c_i, t) \quad \Rightarrow \quad \hat{h}_i e^{i\hat{\omega}} = \hat{g}_i(x,t)e^{i\hat{k}c_i}, \tag{3.5}$$

which results in the eigenvalue problem as found in ref. [4],

$$\frac{1}{3} \begin{bmatrix} e^{-i\hat{k}}(3 - 1/\tau) & e^{-i\hat{k}}/2\tau & -e^{-i\hat{k}}/\tau \\ 2/\tau & 3 - 1/\tau & 2/\tau \\ -e^{i\hat{k}}/\tau & e^{i\hat{k}}/2\tau & e^{i\hat{k}}(3 - 1/\tau) \end{bmatrix} \begin{bmatrix} \hat{h}_- \\ \hat{h}_0 \\ \hat{h}_+ \end{bmatrix} = e^{i\hat{\omega}} \begin{bmatrix} \hat{h}_- \\ \hat{h}_0 \\ \hat{h}_+ \end{bmatrix}. \tag{3.6}$$

Through assuming $\hat{k} = k$ known and finding the eigenvalue $\mathrm{e}^{\mathrm{i}\hat{\omega}}$ numerically, we may study the behaviour of temporally damped waves in the LBM. Alternatively, we may assume $\hat{\omega} = \omega$ known and find the value of $\hat{k}$ which gives the correct eigenvalue $\mathrm{e}^{\mathrm{i}\omega}$ through a nested binary search in k' and α_x. This allows us to study the behaviour of spatially damped waves also.

The eigenvector itself may be used to determine the relative complex amplitudes $\hat{\rho}'$ and $\rho_0\hat{u}'$ of the density and velocity waves. It may be found from eqs. 2.4 and 3.3 that $\hat{\rho}' = \hat{h}_- + \hat{h}_0 + \hat{h}_+$ and $\rho_0\hat{u}' = \hat{h}_+ - \hat{h}_-$, so that

$$\frac{\rho_0\hat{u}'}{\hat{\rho}'} = \frac{\hat{h}_+ - \hat{h}_-}{\hat{h}_- + \hat{h}_0 + \hat{h}_+}. \tag{3.7}$$

In this way we may compare the ratios of the LB amplitudes with theoretical ones from eq. 2.7a.

4. Results

We may validate the linearization method by comparing with actual LB simulations. A spatially damped plane wave may be created in a simple fashion in a D1Q3 lattice by pinning density and velocity to small sinusoidal functions around an equilibrium, setting $\rho(0, t) = \rho_0 + |\hat{\rho}'|\sin(\omega t)$, $u(0, t) = |\hat{u}'|\sin(\omega t + \angle[\hat{u}'/\hat{\rho}'])$ in the first node and always relaxing it to equilibrium. We may then measure the phase velocities and absorption coefficients of the resulting waves.

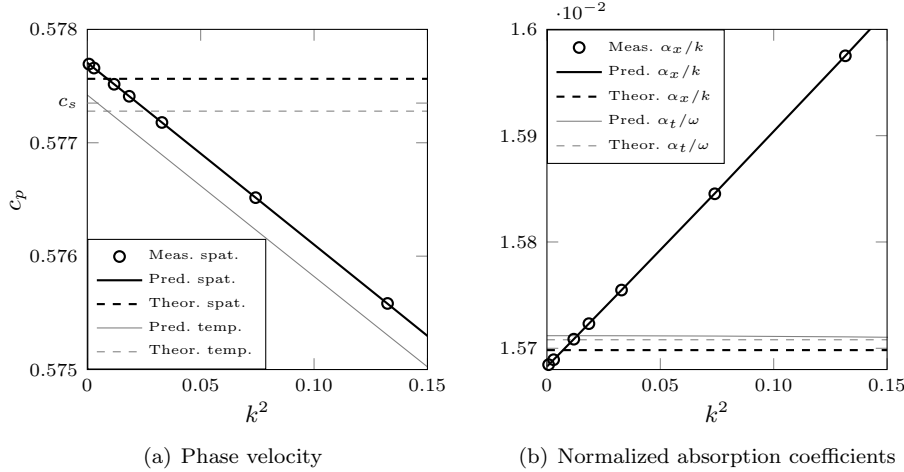(a) Phase velocity   (b) Normalized absorption coefficients

Figure 1. Comparison of predicted LB and measured phase velocity and normalized absorption coefficients for spatially and temporally damped waves at $\omega\tau_\nu = 2\pi \times 5 \times 10^{-3}$ with theoretical values from eqs. 2.5 and 2.6.

The comparison is performed in Figure 1, where we also compare with theoretical values. We see that the linearization analysis for spatially damped waves accurately predicts the values measured from simulations, validating this method as a tool for predicting the behaviour of spatially damped waves. Validation for temporally damped waves has already been performed [4]. From this point, we will therefore use the linearization analysis to study the behaviour of LB waves.

The theoretical values in eqs. 2.5 and 2.6 change only with the dimensionless parameter $\omega\tau_\nu$. Our analysis shows that the LB phase velocity has a small numerical dispersion which for low k is linear in k^2. This k^2 error also affects the spatial absorption coefficient, while the temporal absorption coefficient is hardly influenced in this way, being instead mainly affected by a very small k^4 error.

In addition, the values for the phase velocity and absorption coefficients do not agree even when the numerical resolution goes to infinity (the $k \to 0$ limit), which means that the LBM with the BGK operator does not appear to be a consistent method for simulating waves. We will now examine how the waves behave in this limit.
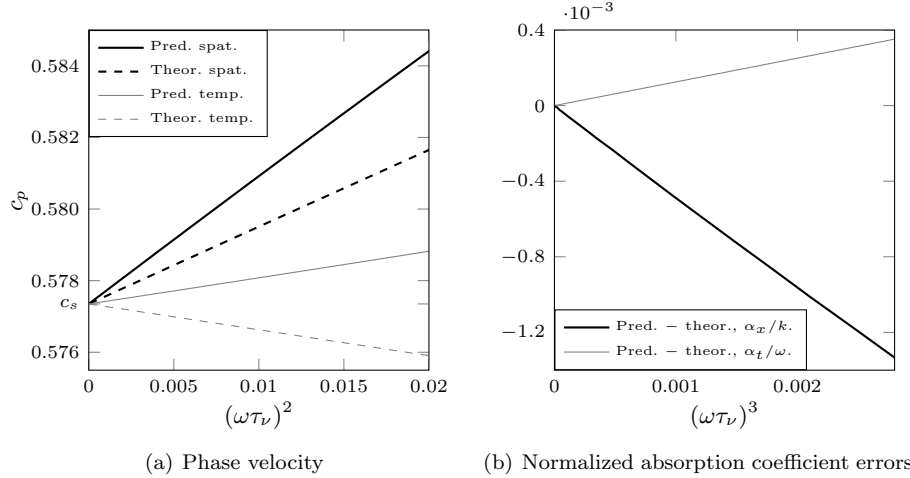

(a) Phase velocity   (b) Normalized absorption coefficient errors

Figure 2. Comparison of predicted LB and theoretical phase velocity and normalized absorption coefficients in $k \to 0$ limit as function of $\omega\tau_\nu$.

Figure 2 compares the behaviour of LB waves in this limit with theoretical behaviour. We find an agreement with theory and Chapman-Enskog analysis in the $k \to 0$, $\omega\tau_\nu \to 0$ limit for both phase velocity and absorption. The phase velocity is a linear function of $(\omega\tau_\nu)^2$ as expected, but the slope is too steep in both cases. The absorption is correct apart from some small errors in $(\omega\tau_\nu)^3$.

Finally, we compare the ratio $\rho_0\hat{u}'/\hat{\rho}'$, as given from theory (eq. 2.7a) and as predicted through the linearization analysis (eq. 3.7). From Figure 3, we see that the amplitudes of the waves are linear functions of $(\omega\tau_\nu)^2$, but that the slope of spatially and temporally damped waves are again both steeper than they should be. The phase shift is largely correct, with a small $(\omega\tau_\nu)^3$ error for spatially damped waves and an insignificant $(\omega\tau_\nu)^5$ error for temporally damped waves. Again, the results agree with theory in the $k \to 0$, $\omega\tau_\nu \to 0$ limit.

We have seen that the waves' properties are quite well-behaved, although not necessarily correct. Table 1 compares the LB and theoretical properties of the waves we have studied in the $k \to 0$ limit, with terms of order $\mathcal{O}([\omega\tau_\nu]^3)$ or higher neglected. We find that the while the normalized absorption coefficients and phase shifts are consistent with theory in this limit, the phase velocities and amplitude ratios do not match except in the inviscid limit. In fact, both of these increase at rates which are $(\omega\tau_\nu)^2/4$ greater than they should be.
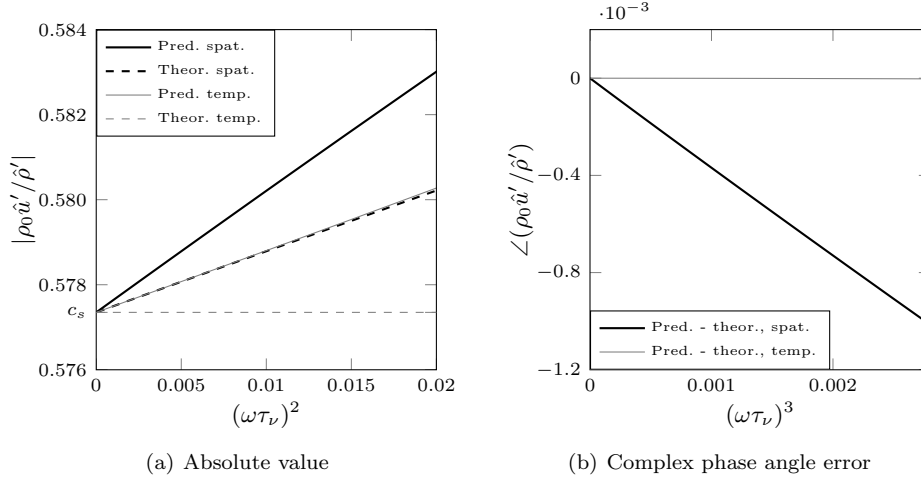
(a) Absolute value

(b) Complex phase angle error

Figure 3. Comparison of predicted LB and theoretical ratio between the complex wave amplitudes $\rho_0 \hat{u}'$ and $\hat{\rho}'$.

Table 1. *Wave properties in the $k \to 0$, small $\omega\tau_\nu$ limit*

(Tabulation of the predicted LB and theoretical properties of spatially and temporally damped waves at infinite resolution ($k \to 0$) when $\omega\tau_\nu$ is small. $\alpha_*/*$ indicates normalized absorption coefficient for both types of damped waves.)

Type	c_p/c_s	$\alpha_*/*$	$|\rho_0\hat{u}'/\hat{\rho}'|/c_s$	$\angle(\rho_0\hat{u}'/\hat{\rho}')$
Predicted spatial	$1 + \frac{5}{8}(\omega\tau_\nu)^2$	$\omega\tau_\nu/2$	$1 + \frac{1}{2}(\omega\tau_\nu)^2$	$\omega\tau_\nu/2$
Theoretical spatial	$1 + \frac{3}{8}(\omega\tau_\nu)^2$	$\omega\tau_\nu/2$	$1 + \frac{1}{4}(\omega\tau_\nu)^2$	$\omega\tau_\nu/2$
Predicted temporal	$1 + \frac{1}{8}(\omega\tau_\nu)^2$	$\omega\tau_\nu/2$	$1 + \frac{1}{4}(\omega\tau_\nu)^2$	$\omega\tau_\nu/2$
Theoretical temporal	$1 - \frac{1}{8}(\omega\tau_\nu)^2$	$\omega\tau_\nu/2$	1	$\omega\tau_\nu/2$

5. Conclusion

We have examined the behaviour of viscously damped LB waves using the BGK collision operator. The linearization analysis was shown to be capable of analysing not only temporally damped waves, but also spatially damped waves.

We found that while the absorption coefficients and phase shifts match theory well, the phase velocities and amplitude ratios do not, except in the limit of an inviscid lossless fluid. The results are valid for plane waves propagating along a main axis in any lattice for which D1Q3 is a projection. The BGK operator allows no freedom to affect this, so addressing this problem would require an alternate method. On the other hand, the actual behaviour in the infinite resolution limit $k \to 0$ has been quantified in Table 1, and the regularity of the deviations makes it quite possible to predict LB phase velocities and absorption coefficients *a priori* [11].

Since there is no independent pressure wave in the LBM, it is not possible to perform comparisons with eq. 2.7b. In fact, the Chapman-Enskog analysis for the LBM assumes that $p = c_s^2\rho$, which may be shown from eq. 2.7 to be incorrect for damped acoustic waves. That this incorrect assumption underlies the LBM may be a reason for the systematic deviations from theory which we have seen here.

However, an extended energy-conserving LBM has been proposed [12], and has been validated for a number of compressible flow problems [13]. Perhaps this method would give results more consistent with theory.

The deviations are still quite small, and have been found to be comparable to the ones found for high-order finite difference schemes [14]. They also found the LBM to be faster than high-order methods of similar accuracy. This indicates that the LBM is a promising tool for CAA.

In this article, we have only looked at the effects of viscosity on damped acoustic waves. In real fluids, there are very significant contributions to this damping from thermal conduction and molecular relaxation [6,15]. It remains to be seen how the LBM may be adapted to handle all three damping mechanisms.

References

1 Lighthill, M. J. 1952 On sound generated aerodynamically. I. General theory. *Proc. R. Soc. Lond. A* **211**, 564–587

2 Popescu, M. & Johansen, S. T 2009 Modelling of aero-acoustic wave propagation in low Mach number corrugated pipe flow. *Prog. Comp. Fluid Dyn.* **9**, 417–425

3 Chen, S & Doolen, G. D. 1998 Lattice Boltzmann method for fluid flows. *Annu. Rev. Fluid Mech.* **30**, 329–364

4 Dellar, P. J. 2001 Bulk and shear viscosities in lattice Boltzmann equations. *Phys. Rev. E* **64**, 031203

5 Lallemand, P. & Luo, L-S. 2000 Theory of the lattice Boltzmann method: Dispersion, dissipation, isotropy, Galilean invariance, and stability. *Phys. Rev. E* **61**, 6546–6562

6 Kinsler, L. E., Frey, A. R, Coppens, A. B. & Sanders, J. V 2000 *Fundamentals of acoustics*, ch. 8, 4th edn. John Wiley & Sons.

7 Hamilton, M. F. & Morfey, C. L. 1998 Model equations. In *Nonlinear acoustics* (ed. Hamilton, M. F. & Blackstock, D. T.). Academic Press.

8 Buick, J. M., Greated, C. A. & Campbell, D. M. 1998 Lattice BGK simulation of sound waves. *Europhys. Lett.* **43**, 235–240

9 Brès, G. A., Pérot, F. & Freed, D. 2009 Properties of the lattice-Boltzmann method for acoustics. In *15th AIAA/CEAS Aeroacoustics Conference*

10 Wagner, A. J. 2006 Thermodynamic consistency of liquid-gas lattice Boltzmann simulations. *Phys. Rev. E* **74**, 056703

11 Viggen, E. M. 2010 The lattice Boltzmann method in acoustics. In *33rd Scandinavian Symposium on Physical Acoustics*

12 Prasianakis, N. I. & Karlin, I. V. 2007 Lattice Boltzmann method for thermal flow simulation on standard lattices. *Phys. Rev. E* **76**, 016702

13 Prasianakis, N. I. & Karlin, I. V. 2008 Lattice Boltzmann method for simulation of compressible flows on standard lattices. *Phys. Rev. E* **78**, 016704

14 Marié, S., Ricot, D. & Sagaut, P. 2009 Comparison between lattice Boltzmann method and Navier-Stokes high order schemes for computational aeroacoustics. *J. Comp. Phys.* **228**, 1056–1070

15 Blackstock, D.T. 2000 *Fundamentals of physical acoustics*, ch. 9, 1st edn. John Wiley & Sons